Local structure, chemical bond parameters and hyperfine magnetic interactions of ^{57}Fe and doped ^{119}Sn atoms in the orthoferrites $TlFeO_3$ and $TlFe_{0.99}Sn_{0.01}O_3$

2006 J. Phys.: Condens. Matter 18 8943

(http://iopscience.iop.org/0953-8984/18/39/024)

INSTITUTE OF PHYSICS PUBLISHING JOURNAL OF PHYSICS: CONDENSED MATTER

J. Phys.: Condens. Matter **18** (2006) 8943–8959 doi:10.1088/0953-8984/18/39/024

Local structure, chemical bond parameters and hyperfine magnetic interactions of ^{57}Fe and doped ^{119}Sn atoms in the orthoferrites $TlFeO_3$ and $TlFe_{0.99}Sn_{0.01}O_3$

I A Presniakov[1], A V Sobolev[1], A V Baranov[1], G Demazeau[2] and V S Rusakov[1]

[1] Department of Chemistry, Lomonosov, Moscow State University, Moscow, Russia
[2] Institut de Chimie de la Matière Condensée de Bordeaux, Bordeaux, France

Received 16 May 2006, in final form 21 July 2006
Published 15 September 2006
Online at stacks.iop.org/JPhysCM/18/8943

Abstract

Mössbauer spectroscopy has been applied to study the magnetic hyperfine interactions of ^{57}Fe and ^{119}Sn probe atoms within $TlFeO_3$ and $TlFe_{0.99}Sn_{0.01}O_3$ ferrites. According to the magnetic measurements, the magnetic ordering temperature T_N (=560 K) for $TlFeO_3$ is much lower than that for any other orthoferrites $RFeO_3$ (R = rare earth). It is suggested that such difference in T_N may be explained by different characteristics of the Tl–O and R–O chemical bonds involved and the induced competition with the Fe–O bonds. The effects of covalency and overlap distortion on the spin and charge densities at ^{57}Fe nuclei are discussed in relation with the hyperfine interactions observed. By using cluster molecular orbital (MO) calculations, it was shown that the low value of the hyperfine magnetic field H_{Fe}(=538 kOe) at ^{57}Fe nuclei in $TlFeO_3$ is strongly associated with a decrease of the covalent mixing parameter $(b_\sigma)^2 = 0.048$ and $(b_\pi)^2 = 0.009$ values, which characterize the Fe–O bond covalence. It was elucidated that the value of super-transferred hyperfine field (H_{STHF}) at ^{119}Sn nuclei in $TlFe_{0.99}Sn_{0.01}O_3$ is sensitive mainly to the angle of the Sn–O–Fe bonds.

1. Introduction

The orthoferrites $RFeO_3$ (R = rare earth) have attracted considerable interest due to the continuous structural distortion and variation of their physical properties from La^{3+} to Lu^{3+} [1], such a phenomenon being induced by the lanthanide contraction correlated to the filling of internal 4f orbitals.

All the $RFeO_3$ perovskites are characterized by the orthorhombic structure belonging to the space group *Pbnm* [1]. In the orthorhombic elementary unit cell, each of the four Fe^{3+}

cations interacts with six nearest Fe^{3+} ions through Fe–O(i)–Fe indirect bonds of two adjacent FeO_6 octahedra. According to the symmetry of the space group *Pbnm*, two kinds of these bonds can be found. The first Fe–O(4c)–Fe bond is directed along the *c*-axis of the crystal and the second one, Fe–O(8d)–Fe, is within the *ab*-plane forming super-exchange angles ϑ_1 and ϑ_2, respectively. For the light R^{3+} ions (La–Gd), the ϑ_1 and ϑ_2 angles are almost equal. However, for orthoferrites of heavy R^{3+} ions, the difference in the magnitudes of ϑ_1 and ϑ_2 is nearly 1°–1.5°, although the average Fe–O distance remains constant in all the ferrites of the $RFeO_3$ series [1].

The distortion of the FeO_6 octahedra is not so important but the tilting between shared corner octahedra decreases from La^{3+} to Lu^{3+} and consequently the average Fe–O–Fe angle ϑ is continuously reduced from 157.3° to 141.8° [2]. Consequently, the overlap between $3d_{\sigma,\pi}$ (Fe^{3+}) and $2p_{\sigma,\pi}$ (O^{2-}) orbitals is reduced leading to a weakening of the magnetic interactions: from T_N ($LaFeO_3$) = 740 K to T_N ($LuFeO_3$) = 623 K [2].

Another example of the variation of physical properties along an RMO_3 perovskite series is the modification of the electronic localization of e_g electron versus R^{3+} for the $RNi^{3+}O_3$ perovskites (low spin Ni^{3+}: $t_{2g}^6e_g^1$). If $LaNiO_3$, characterized by a weak structural distortion (rhombohedral structure with the average ϑ value close to 180°), presents a metallic behaviour [3, 4], the electronic localization is improved when the ϑ angle is reduced: such an improvement of the localization induces an electronic instability leading to the disproportionation [$2Ni^{3+} \rightarrow Ni^{(3+\varepsilon)+} + Ni^{(3-\varepsilon)+}$]. Such a phenomenon has been recently emphasized both by neutron diffraction [5] and Mössbauer spectroscopy (using ^{57}Fe as the Mössbauer probe) [6].

Therefore, it was interesting to evaluate the lattice structural distortion and consequently its influence on the resulting physical properties of the $AFeO_3$ perovskite with A^{3+} different to a rare earth element ($R^{3+} = Tl^{3+}$).

Recently [7], a polycrystalline $TlFeO_3$ sample was prepared under high pressure–high temperature conditions with a 'belt' type apparatus and it was characterized using powder x-ray diffraction and magnetic measurements. It was shown that as well as the $RFeO_3$ (R = rare earth), $TlFeO_3$ is characterized by the orthorhombic structure with a $\langle\vartheta\rangle = 144°$ value which is comparable to that for $ErFeO_3$ [7]. However, in spite of the almost exact coincidence of the geometrical parameters of the Fe–O–Fe 'super-exchange' bonds for these two ferrites ($TlFeO_3$ and $ErFeO_3$), the magnetic ordering temperature of $TlFeO_3$ ($T_N = 560$ K) is much lower than that for $ErFeO_3$ ($T_N = 643$ K). It is notable that the analogical tendency for the T_N behaviour, when R^{3+} is substituted for Tl^{3+}, was observed for $TlNiO_3$ and $RNiO_3$ [8]. It was suggested [7] that the low values of T_N for $TlFeO_3$ and $TlNiO_3$ are due to the electronic structure of Tl^{3+} cations, which are able to form stronger covalent Tl–O bonds. As a result of the electron density shift Fe → O → Tl, there occurs an increase of the ionic character for the Fe–O bonds. In turn, the weakening of the indirect Fe–O–Fe interactions is observed and therefore the values of T_N for $TlFeO_3$ and $TlNiO_3$ decrease.

Mössbauer spectroscopy is one of the fruitful methods to investigate the electronic state and crystallographic surroundings of the iron atoms. During the last studies of a great number of iron compounds, it was shown that even a slight change of the Fe–O bond parameters can result in the modification of Mössbauer hyperfine parameters. This paper presents the Mössbauer investigation of the ^{57}Fe atoms in $TlFeO_3$ perovskite in the magnetic ordering ($T < T_N$) domain of temperatures. In addition, the ^{119}Sn Mössbauer spectra for $TlFe_{0.99}Sn_{0.01}O_3$ were recorded and analysed. In the case of magnetically ordered matrices, the ^{119}Sn Mössbauer spectra exhibit Zeeman splitting due to the spin polarization of the diamagnetic probe by its magnetic neighbours. Therefore these magnetic spectra allow getting direct information on the electronic configuration and chemical bonding of the cationic surrounding of the diamagnetic

Mössbauer probe, which generally cannot be done in the case of diamagnetic or paramagnetic matrices. The data obtained are compared with the available data on orthoferrites $RFeO_3$ [9] and $RFe_{0.99}Sn_{0.01}O_3$ [10].

2. Experimental details

2.1. Synthesis and characterization

The synthesis of $TlFeO_3$ has been described in detail elsewhere [7, 11]. The synthesis of ^{119}Sn-doped samples of $TlFe_{0.99}Sn_{0.01}O_3$ involved two stages. In the first stage, tin and iron hydroxides were coprecipitated by an ammonia solution (0.1 M) from acid solutions (pH 3) containing the required amounts of Fe^{3+} and $^{119}Sn^{4+}$ cations. The homogeneous hydroxide mixture thus obtained was dried, ground, and annealed in air until the formation of a $Fe_{1.98}Sn_{0.02}O_3$ solid solution. The composition and the distribution of the ^{119}Sn dopant in $Fe_{1.98}Sn_{0.02}O_3$ were monitored by Mössbauer spectroscopy. In particular, the appearance of a magnetic hyperfine structure in ^{119}Sn spectra is convincing evidence that tin atoms enter into the Fe_2O_3 structure. In the second stage, a thoroughly ground mixture of the precursors $Fe_{1.98}Sn_{0.02}O_3$ and Tl_2O_3 was thoroughly mixed and encapsulated in a gold tube. The capsule was separated from the graphite tube used as a microfurnace by a layer of NaCl powder and then heated at 850 °C under 7 GPa for 30 min [7]. The annealing was continued until x-ray powder diffraction confirmed the formation of single-phase ferrites.

The magnetization was measured with a Faraday-type DSM-8 magnetometer in the temperature range from 300 to 750 K at 1.7 T.

The ^{57}Fe and ^{119}Sn Mössbauer spectra were recorded at 77–300 K using a conventional constant-acceleration spectrometer. The radiation sources ^{57}Co(Rh) and $Ca^{119m}SnO_3$ were kept at room temperature. All isomer shifts refer to the α-Fe (^{57}Fe spectra) and $CaSnO_3$ (^{119}Sn) absorbers at 300 K. The experimental spectra were processed and analysed with the MSTools package [12].

2.2. Calculation of covalency effects on the magnetic hyperfine field (H_{Fe}) at ^{57}Fe nuclei

For a qualitative discussion of the effects of covalency of the Fe^{3+}–O bonds on the magnetic hyperfine field (H_{Fe}) at the Fe^{3+} sites in the $TlFeO_3$ structure we used a simple model of constructing group molecular orbitals (MOs) for a cluster $\{Fe(O_6Fe_6)\}$ (figure 1(a)). In this cluster, the central Fe^{3+} cation is antiferromagnetically coupled to its six nearest iron neighbours through Fe–O–Fe bonds (a G-type of magnetic structure). A general algorithm for the semi-quantitative analysis of the various covalency parameters using a proper linear combination of atomic orbitals (LCAO) was first proposed for the spinel ferrites [13] and the orthoferrites [14]. In particular, it was shown that consideration of different mechanisms of 'covalency effects' allows one to represent the experimental H_{Fe} value as a sum of several independent contributions:

$$H_{Fe} = H_F + \Delta H_{red} + \Delta H_{cov} + \Delta H_{STHF}, \tag{1}$$

where H_F is the hyperfine field for a free Fe^{3+} cation; ΔH_{red} (<0) is the contribution caused by the influence of the Fe^{3+}–O bond covalency on the population of the Fe^{3+} 3d orbitals; ΔH_{cov} (<0) is the covalent contribution due to the participation of the core ns orbitals (n = 1–3) and the valence 4s orbitals of the Fe^{3+} cation in the Fe–O bonds (the positive and negative signs indicate that a given covalent contribution leads to an increase (>0) or decrease (<0) of the overall H_{Fe} field magnitude); ΔH_{STHF} is the super-transferred hyperfine field induced at the central Fe^{3+} cation by its neighbouring iron cations.

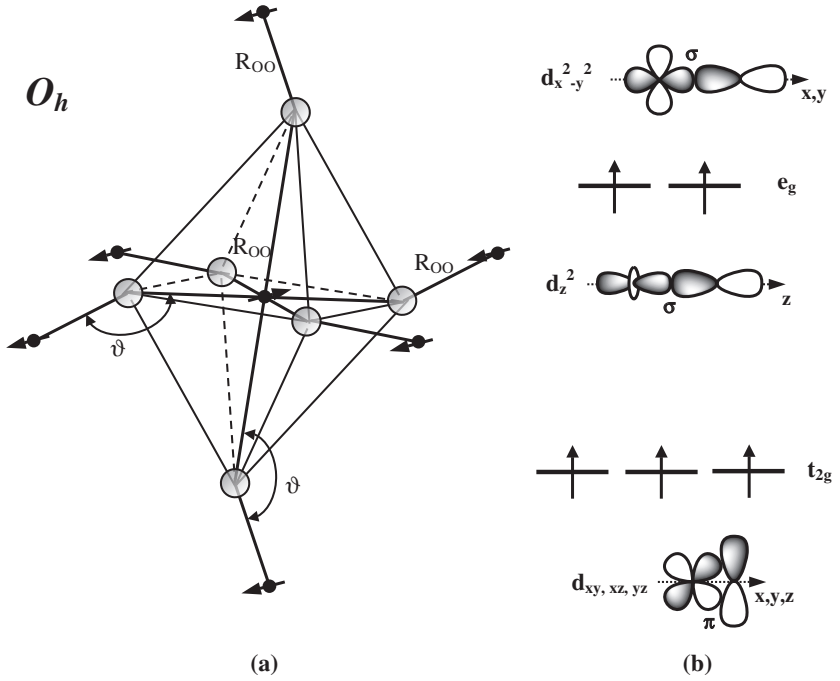

Figure 1. $Fe(O_6Fe_6)$ ideal cluster (a) and a corresponding scheme of the 3d atomic orbitals splitting (b).

In the purely ionic iron compounds the hyperfine structure of Fe^{3+} cations is mainly affected by their nearest neighbouring oxygen anions; it suffices to consider only the bonding MOs, which are predominantly localized at more electronegative oxygen atoms:

$$\Psi_{\mathrm{d}}^{\uparrow(\downarrow)} = N_{\mathrm{d}}^{\uparrow(\downarrow)}\{L_{\mathrm{s,p}}^{\uparrow(\downarrow)} + D_{(\mathrm{s,p-d})}^{\uparrow(\downarrow)}\varphi_{\mathrm{d}}^{\uparrow(\downarrow)}\} \tag{2}$$

$$\Psi_{\mathrm{s}}^{\uparrow(\downarrow)} = N_{\mathrm{s}}^{\uparrow(\downarrow)}\left\{L_{\mathrm{s,p}}^{\uparrow(\downarrow)} + \sum_{n=1}^{4} D_{(\mathrm{s,p}-ns)}^{\uparrow(\downarrow)}\varphi_{ns}^{\uparrow(\downarrow)} + D_{(\mathrm{s,p-d})}^{\uparrow(\downarrow)}\Phi_{\mathrm{d}}^{\uparrow(\downarrow)}\right\}. \tag{3}$$

The first group of MOs described by equation (2) accounts for the covalency effects on the population of the 3d orbitals of the central Fe^{3+} cation in the $\{Fe(O_6Fe_6)\}$ cluster. These MOs are represented by a linear combination of the 3d atomic orbitals (AOs) of the Fe^{3+} cation ($\varphi_{\mathrm{d}}^{\uparrow(\downarrow)}$) transformed according to the corresponding irreducible representation of the point group of the cluster, as well as of the group orbitals ($L_{\mathrm{s,p}}^{\uparrow(\downarrow)}$) made up of the 2s or 2p orbitals of oxygen. The ↑ (↓) symbols denote the positive and negative directions of spins; the direction of the overall spin for the unpaired 3d electrons of the central Fe^{3+} cation was taken to be positive (↑) (figure 1(a)).

According to the scheme in figure 2(a), the covalency effect with the participation of the 3d orbitals of the central Fe^{3+} cation corresponds to a virtual transfer of an electron from the filled $L_{\mathrm{s,p}}^{\downarrow}$ orbitals to the vacant $\varphi_{\mathrm{d}}^{\downarrow}$ orbitals. Inasmuch as the spin of the electron transferred is opposite to the Fe^{3+} spin (↑), this transfer leads to a decrease in the magnetic moment of Fe^{3+} and therefore results in a reduction of the experimental H_{Fe} field by ΔH_{red} (<0) value (figure 2(a)). This effect can be quantified with the use of the $D_{(\mathrm{s,p-d})}^{\uparrow(\downarrow)}$ parameters from equation (2); the physical meaning of these parameters depends on the population of

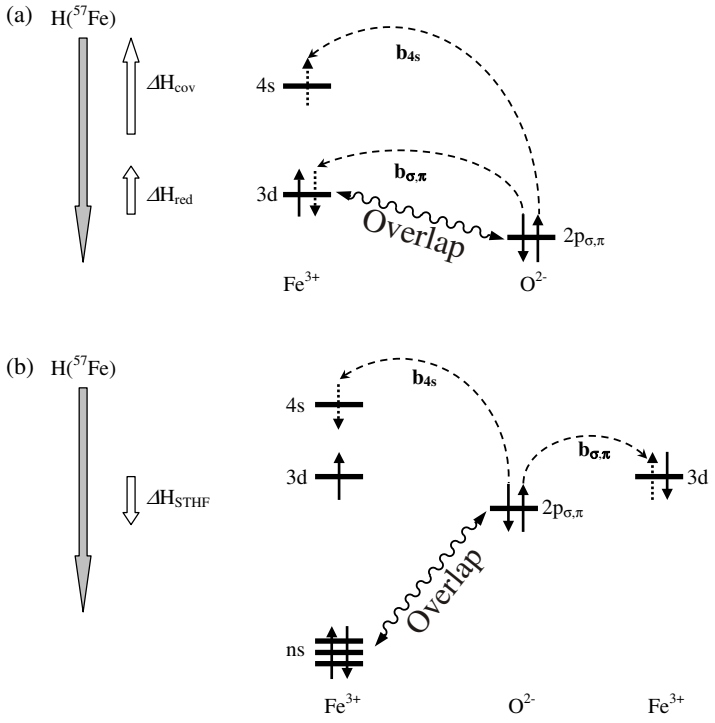

Figure 2. Scheme of hyperfine magnetic field $\Delta H_{\rm red}$, $\Delta H_{\rm cov}$ and $\Delta H_{\rm STHF}$ contributions at $^{57}Fe^{3+}$ in $Fe(O_6Fe_6)$ clusters.

the corresponding 3d orbitals:

$$D^{\uparrow(\downarrow)}_{\rm s,p-d} = \begin{cases} -S_{\rm s,p} & \text{for occupied } (\uparrow) \text{ 3d orbitals} \\ B_{\rm (s,p-d)} & \text{for vacant } (\downarrow) \text{ 3d orbitals,} \end{cases} \tag{4}$$

where $B_{\rm (s,p-d)}$ is the group covalent mixing parameter describing the electron transfer from the $L^{\downarrow}_{\rm s,p}$ orbital of O^{2-} anions to the vacant $\varphi^{\downarrow}_{\rm d}$ orbitals of Fe^{3+}; $S_{\rm (s,p-d)}$ is the group overlap integral for the $L^{\uparrow}_{\rm s,p}$ orbitals and the filled $\varphi^{\uparrow}_{\rm d}$ orbitals.

Using equation (2) for MOs and expressing the $D^{\uparrow(\downarrow)}_{\rm (s,p-d)}$ parameters in terms of equation (4), we obtain the final formula for the $\Delta H_{\rm red}$ contribution:

$$\Delta H_{\rm red} = \tfrac{1}{5} H_{\rm F} \sum_{\rm d} [\{N^{\uparrow}_{\rm d} S_{\rm (s,p-d)}\}^2 - \{N^{\downarrow}_{\rm d} B_{\rm (s,p-d)}\}^2], \tag{5}$$

where $N^{\uparrow(\downarrow)}_{\rm d}$ stands for the normalization constants that can be obtained from the procedure of orthogonalization of the MOs (2):

$$N^{\uparrow}_{\rm d} = \left(1 + R_{\rm (s,p-s,p)} - S^2_{\rm (s,p-d)}\right)^{-1/2} \tag{6a}$$

$$N^{\downarrow}_{\rm d} = \left(1 + R_{\rm (s,p-s,p)} + B^2_{\rm (s,p-d)} + 2B_{(s,p-d)} S_{\rm (s,p-d)}\right)^{-1/2}, \tag{6b}$$

where $R_{\rm (s,p-s,p)}$ is determined by the oxygen–oxygen overlap integrals of the $L^{\uparrow(\downarrow)}_{\rm s,p}$ group orbitals; $H_{\rm F} = 630$ kOe is the magnetic hyperfine field (Fermi contact field) for the hypothetical case of a free iron cation [13].

The second group of MOs represented by equation (3) is used for considering the direct effect of covalency of the Fe–O bonds on the ns-electron (n = 1–4) spin density distribution at the Fe^{3+} nucleus. In addition to the ns atomic orbitals (φ_{ns}) of the central Fe^{3+} cation and the group $L_{s,p}^{\uparrow(\downarrow)}$ orbitals of its nearest neighbouring O^{2-} anions, equation (3) contains the group orbitals $\Phi_{d}^{\uparrow(\downarrow)}$ composed of the 3d orbitals of the Fe^{3+} cation that form the second coordination sphere in the {Fe(O_6Fe_6)} cluster. These cations lead to spin polarization of the O^{2-} orbitals which can be quantified with the use of the $D_{(s,p-ns)}^{\uparrow(\downarrow)}$ parameters determined by the population of the ns orbitals (n = 1–4) of the central Fe^{3+} cations:

$$D_{(s,p-ns)}^{\uparrow(\downarrow)} = \begin{cases} -S_{(s,p-ns)}^{\uparrow(\downarrow)} & \text{for occupied } ns \text{ orbitals } (n = 1\text{–}3) \\ B_{(s,p-4s)}^{\uparrow(\downarrow)} & \text{for vacant 4s orbital,} \end{cases} \tag{7}$$

where $B_{(s,p-4s)}$ is the covalent mixing parameter describing the electron transfer from the $L_{s,p}$ orbitals of O^{2-} to the vacant 4s orbital of the central Fe^{3+} cation; $S_{(s,p-d)}$ is the group overlap integral of the filled ns orbitals (n = 1–3) of the Fe^{3+} cation and the $L_{s,p}$ orbitals of its surrounding O^{2-} anions.

The general expressions for the ΔH_{cov} and ΔH_{STHF} terms can be written with the use of wavefunctions (3):

$$\Delta H_{cov} = \frac{8\pi}{6}\mu_B(\{N_s^{\uparrow}\}^2 + \{N_s^{\downarrow}\}^2)\sum_{n=1}^{4}(\{D_{(s,p-ns)}^{\downarrow}\varphi_{ns}^{\downarrow}(0)\}^2 - \{D_{(s,p-ns)}^{\uparrow}\varphi_{ns}^{\uparrow}(0)\}^2), \tag{8}$$

$$\Delta H_{STHF} = \frac{8\pi}{6}\mu_B(\{N_s^{\uparrow}\}^2 - \{N_s^{\downarrow}\}^2)\sum_{n=1}^{4}(\{D_{(s,p-ns)}^{\uparrow}\varphi_{ns}^{\uparrow}(0)\}^2 + \{D_{(s,p-ns)}^{\downarrow}\varphi_{ns}^{\downarrow}(0)\}^2), \tag{9}$$

where $8\pi\mu_B/3$ (=525 kOe) and μ_B is the electron Bohr magneton.

The ΔH_{cov} contribution appears because the transfer ($B_{(s,p-4s)}^{\uparrow} > B_{(s,p-4s)}^{\downarrow}$) and overlap ($S_{(s,p-ns)}^{\uparrow} > S_{(s,p-ns)}^{\downarrow}$ (n = 1, 2); $S_{(s,p-3s)}^{\uparrow} < S_{(s,p-3s)}^{\downarrow}$) parameters in the expression for $D_{(s,p-ns)}^{\uparrow(\downarrow)}$, as well as the values of the spin-polarized wavefunctions $\varphi_{ns}^{\uparrow}(0)$ and $\varphi_{ns}^{\downarrow}(0)$ at the ^{57}Fe nuclei, depend on the direction of the total spin of the reference Fe^{3+} cations. In the analysis of the sign of ΔH_{cov}, it should be taken into account that the $O^{2-} \rightarrow Fe^{3+}$ electron transfer mainly leads to the population of the spin-polarized $4s^{(\uparrow)}$ orbitals of the iron cations, which have the same direction of the spin as their own 3d electrons. Therefore, the uncompensated 4s spin density that emerges at the Fe^{3+} nuclei will have the opposite sign with respect to the spin density of the core ns electrons induced due to their Fermi contact interaction with unpaired 3d electrons [8, 10]. This means that the inclusion of the covalent contribution ΔH_{cov} leads to a decrease in the overall hyperfine field H_{Fe} (figure 2(a)).

The physical meaning of the ΔH_{STHF} contribution, described by equation (9), is determined by the difference between the normalization constants $(N_s^{\uparrow})^2$ and $(N_s^{\downarrow})^2$ in this expression. Using equation (9), and taking that $\{D_{(s,p-ns)}^{\uparrow}\}^2 \approx \{D_{(s,p-ns)}^{\downarrow}\}^2$, we can write an approximate expression suitable for further analysis:

$$\{N_s^{\uparrow}\}^2 - \{N_s^{\downarrow}\}^2 \approx A_{(s,p-d)}^2\{N_s^{\uparrow}N_s^{\downarrow}\}^2 \tag{10}$$

where $A_{(s,p-d)}^2 = (B_{(s,p-d)} + S_{(s,p-d)})^2$ is the covalent mixing parameter corresponding to the $Fe^{3+} \rightarrow O^{2-}$ spin transfer (spin polarization) involving the iron cations from the second coordination sphere of the {Fe(O_6Fe_6)} cluster. As a result of spin polarization, the group $L_{s,p}^{\uparrow(\downarrow)}$ orbitals gain a fraction of the unpaired spin density ($\sim A_{(s,p-d)}^2$), some part of which ($\sim S_{(s,p-ns)}^2 A_{(s,p-d)}^2$) is transferred to the ns orbitals of the central Fe^{3+} cation due to the overlap and covalence effects. The sign of the spin density thus transferred is determined by the direction of the spins of the paramagnetic neighbours

surrounding the central iron cation. Taking into account that, for an antiferromagnetically ordered structure of the G-type (figure 1), the direction of the magnetic moments of all iron cations in the second coordination sphere of the $\{Fe(O_6Fe_6)\}$ cluster is opposite to the direction of the magnetic moment of the central Fe^{3+} cation (figure 2(b)), the super-transferred hyperfine field ΔH_{STHF} should enter into equation (1) with a positive sign.

In order to reduce the number of the unknown MO parameters in equations (5), (8) and (9), we made some assumptions.

(1) Among the valence orbitals of O^{2-} anions, only the 2p orbitals were taken into account. This assumption is based on the significant difference between the radial distribution functions for the 2s and 2p AOs and, as a result, between the overlap integrals of these orbitals with the valence 3d and ns orbitals of Fe^{3+} cations: $S_{(s-d)} \ll S_{(p-d)}$ and $S_{(s-ns)} \ll S_{(p-ns)}$. Analogous inequalities can be written for the parameters characterizing the degree of the $O^{2-} \rightarrow Fe^{3+}$ electron transfer: $B_{(s-d)} \ll B_{(p-d)}$ and $B_{(s-ns)} \ll B_{(p-ns)}$. Thus, all terms in equations (5), (8) and (9) containing the overlap integrals $S_{(s-d)}(S_{(s-ns)})$ and covalent transfer parameters $B_{(s-d)}(B_{(s-ns)})$ can be neglected.

(2) It was assumed that the nearest oxygen environment of the central Fe^{3+} cations in the $\{Fe(O_6Fe_6)\}$ clusters is a regular octahedron (point group O_h) with six equivalent bonds, $\langle Fe\text{–}O\rangle = 2.131$ Å [7]. For the anionic environment with point symmetry O_h, the five initially degenerate 3d orbitals of the Fe^{3+} cation are split into two subgroups corresponding to the irreducible representations e_g (σ bonds) and t_{2g} (π bonds) (figure 1(b)). Each group of the e_g and t_{2g} orbitals will be characterized by its electron $O^{2-} \rightarrow Fe^{3+}$ transfer (or overlap) parameters B_σ (S_σ) and B_π (S_π), respectively.

(3) To switch from the cluster description, in which the interaction of the central Fe^{3+} cation with its nearest neighbours is described in terms of MOs delocalized over the entire cluster, to the approximate description of this interaction as a sum of the contributions from separate neighbours, the group integrals in equations (2) and (3) should be substituted by the corresponding pairwise parameters. For the central Fe^{3+} cations in an undistorted $\{Fe(O_6Fe_6)\}$ cluster with O_h point symmetry, these rearrangements are as follows:

$$D^{\uparrow(\downarrow)}_{(p-ns)} = \sqrt{6} \cdot d^{\uparrow(\downarrow)}_{ns} \tag{11a}$$

$$D^{\uparrow(\downarrow)}_{(p-\Gamma\mu)} = \begin{cases} d^{\uparrow(\downarrow)}_{\sigma} \cos\vartheta_i & (O_h{:}\Gamma_\mu = e_g) \\ d^{\uparrow(\downarrow)}_{\pi} \sin\vartheta_i & (O_h{:}\Gamma_\mu = t_{2g}). \end{cases} \tag{11b}$$

where d_σ, d_π, and d_{ns} are the pair parameters, whose physical meaning is determined, as in the case of their corresponding group parameters (equations (4) and (7)), by the degree of electron population of the 3d atomic orbitals involved in pairwise interactions Fe–O(i); and ϑ_i is the average super-exchange angle in the Fe–O(i)–Fe linkages.

The substitution of these transformations into equations (5) and (9) gives a convenient representation of the hyperfine contributions ΔH_{red} and ΔH_{STHF} as a sum of the contributions from separate indirect couplings in the $\{Fe(O_6Fe_6)\}$ cluster:

$$\Delta H_{red} \approx \tfrac{1}{5} H_F \sum_{Fe-O_i}^{6} [\{(N^{\alpha}_{d,\sigma} s_{\sigma(i)})^2 - (N^{\beta}_{d,\sigma} b_{\sigma(i)})^2\} + 2\{(N^{\alpha}_{d,\pi} s_{\pi(i)})^2 - (N^{\beta}_{d,\pi} b_{\pi(i)})^2\}] \tag{12}$$

$$\Delta H_{STHF} = 525 \sum_{Fe-O_i}^{6} \left[\left(\sum_{n}^{4} d_{ns} \varphi_{ns}(0) \right)^2 \left(N^4_\sigma a^2_{\sigma i} \cos^2\vartheta_i + N^4_\pi a^2_{\pi i} \sin^2\vartheta_i \right) \right] \tag{13}$$

where $N^4_\sigma \equiv (N^{\alpha}_{s\sigma} N^{\beta}_{s\sigma})^2$ and $N^4_\pi \equiv (N^{\alpha}_{s\pi} N^{\beta}_{s\pi})^2$ are the products of the normalization constants; a_σ ($=b_\sigma + s_\sigma$) and a_π ($=b_\pi + s_\pi$) are the parameters of the Fe^{3+}: $3d^5 \rightarrow O^{2-}$: $2p_{\sigma,\pi}$ local

spin transfer involving the iron cations of the second coordination sphere in the $\{Fe(O_6Fe_6)\}$ clusters.

The first multiplier in equation (13) contains information on the reference cation itself and its pairwise interactions with its nearest anionic environment. The expression for this multiplier includes the characteristics of the reference Fe^{3+} cation in the form of the values of wave atomic functions $\varphi_{ns}(0)$, as well as of the pairwise overlap integrals $s_{ns} \equiv \langle 2p_\sigma | ns \rangle$ and the b_{4s} integrals corresponding to the covalent transfer O^{2-}: $2p_\sigma \rightarrow Fe^{3+}$: $4s^0$

$$\sum_n^4 d_{ns}\varphi_{ns}(0) = \sum_n^3 s_{ns}\varphi_{ns}(0) + b_{4s}\varphi_{4s}(0). \tag{14}$$

The second multiplier, which contains the sum covalent parameters a_σ and a_π, is responsible for the degree of spin polarization of oxygen anions by the paramagnetic iron cations that form the second coordination sphere of the $\{Fe(O_6Fe_6)\}$ clusters. The trigonometric functions in this expression take into account different angular dependences of the pairwise spin transfer integrals for σ- and π-bonding and, thus, determine H_{Fe} as a function of ϑ_i angles in indirect exchange coupling Fe–O(i)–Fe (figure 1(a)).

The integrals $s_{ns}^{\uparrow(\downarrow)}$ in equations (12) and (13) were calculated by means of interpolation of the values of these parameters for different Fe–O distances from [13] by a six-degree polynomial. The values of the spin-polarized wavefunctions $\varphi_{ns}^{\uparrow(\downarrow)}(0)$ were taken from [15] ($n = 1$–3) and [16] ($n = 4$).

3. Results and discussion

3.1. Crystal structure of $TlFeO_3$

The detailed analysis of $TlFeO_3$ crystallographic parameters has been performed in [7]. The most important peculiarity of its crystallographic structure is the Tl^{3+} coordination: 12 Tl–O bond distances can be classified into three groups: (i) four short bonds with 2.225–2.243 Å; (ii) four intermediate bonds with 2.593–2.737 Å; (iii) four long bonds with 3.215–3.381 Å. Such a specific environment around Tl^{3+} can be attributed to the electronic configuration of the Tl^{3+} ion, leading to a bond to oxygen more covalent than that observed for rare earth ions. In fact, there are more (Tl–$O_{(1)}$) and fewer (Tl–$O_{(2)}$) covalent bonds, resulting in considerably more distorted TlO_{12} polyhedra in comparison with RO_{12}.

In our previous paper [7] it was shown that the ratio of the cell parameters, $c/\sqrt{2}a$, can give information about the structural distortion of RO_{12} polyhedra for the perovskite-like oxides RMO_3. The higher the $c/\sqrt{2}a$ value is, the more the distortion of RO_{12} is, and the more the covalent character of the short bonds R–O at the same time as the weakening of the longer R–O bonds. In figure 3 the ionic radius of the R^{3+} cation and the unit cell parameters (a, b, c) are plotted for $RFeO_3$ and $TlFeO_3$. It is observed that $c/\sqrt{2}a$ increases gradually, from $LaFeO_3$ to $LuFeO_3$, according to an increase of the R^{3+} cation 'acidity' for La $\rightarrow$ Lu associated to the shrinking of R^{3+} size. The value $c/\sqrt{2}a = 1.036$ for $TlFeO_3$ is the largest, despite the relatively small Tl^{3+} ionic size, and gives evidence of considerable distortion of (TlO_{12}) polyhedra, resulting from the formation of three strong (Tl–$O_{(1)}$) and three weak (Tl–$O_{(2)}$) bonds.

3.2. Magnetic study of $TlFeO_3$

The temperature dependence of the reciprocal molar magnetic susceptibility is plotted in figure 4. The linear part of $\chi_M^{-1}(T)$ at $T > T_N$ is in a good agreement with Curie–Weiss

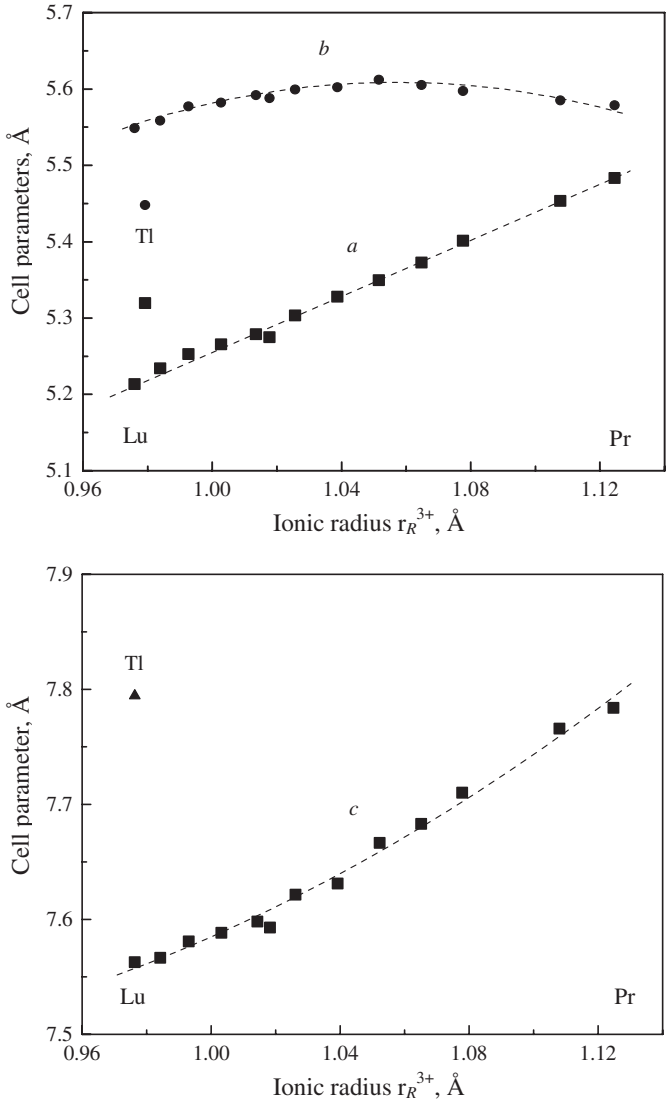

Figure 3. Relation between the ionic radius of the R^{3+} cation and the unit-cell parameters for $TlFeO_3$ and $RFeO_3$ (R = rare earth).

behaviour:

$$1/\chi_M = (T - \Theta)/C_M, \tag{15}$$

where Θ is the paramagnetic Curie temperature, and C_M is the Curie constant. After linear extrapolation of the $\chi_M^{-1}(T)$ dependence ($T > T_N$) the following values were found: $\Theta = -1287$ K and $C_M = 2.30$. From the experimental value of C_M the value of the effective magnetic moment was estimated to be 6.5 μ_B, which is very close to the spin-only value (5.9 μ_B) for the high-spin Fe^{3+} ($2\sqrt{S(S+1)}\ \mu_B = 5.9\ \mu_B$, $S = 5/2$).

The temperature dependence of $\chi_M^{-1}(T)$ shows an abrupt change around 560 K (T_N). This value is much lower than T_N value (=640–715 K) observed for the orthoferrites $RFeO_3$ [1].

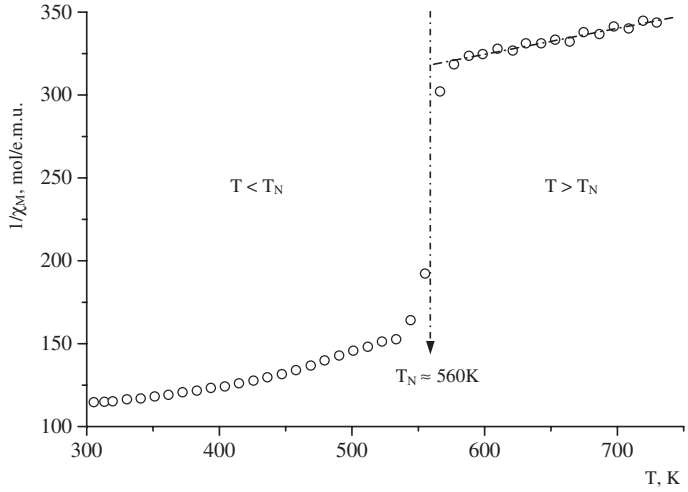

Figure 4. Temperature dependence of the reciprocal magnetic susceptability for $TlFeO_3$.

Before explaining such difference, it should be noted that T_N for insulators is due to the exchange integral (J_m) which characterizes the strength of the magnetic interactions between transition metal M^{m+} cations [17]:

$$T_N = -\Theta = -\frac{2S(S+1)}{3k}\sum_m z_m J_m, \tag{16}$$

where S is the total spin of $M^{m+}(d^n)$; k is Boltzman constant; z_m is the number of the nearest magnetic cations of each type (Σ for all magnetically non-equivalent cations).

The magnitude and sign of the integral J depend on the electronic configuration of the magnetic cation M^{m+} (d^n), parameters of the chemical bond M^{m+}–O, and the geometry of M^{m+}–O–M^{m+} chains. It was shown in [18] that for the indirect interaction between isovalent M^{m+} cations, the exchange integral (J_{MOM}) can be written as follows:

$$J_{MOM} = \sum_{\sigma,\pi}\left(b^4_{\sigma,\pi}\frac{\Delta^2}{U} + \frac{1}{2}b^4_{\sigma,\pi}\Delta\right)\beta^2_{\sigma,\pi}, \tag{17}$$

where $b_{\sigma,\pi} \equiv \langle p_{\sigma,\pi}|h|d_{\sigma,\pi}\rangle$ is the pair σ- and π-type covalent mixing parameters between the $2p_{\sigma,\pi}(O^{2-})$- and $d_{\sigma,\pi}(M^{m+})$-orbitals, $(\beta_{\sigma,\pi})^2$ the geometrical contribution due to the deviation of the M–O–M angle from 180° ($\beta^2_\sigma \sim \cos^2\vartheta$ and $\beta^2_\pi \sim \sin^2\vartheta$), Δ is the $2p^6(O^{2-}) \rightarrow d^{n+1}(M^{(m-1)+})$ charge transfer energy, and U is the $d^n(M^{m+}) + d^n(M^{m+}) \rightarrow d^{n-1}(M^{(m+1)+}) + d^{n+1}(M^{(m-1)+})$ electron transfer energy; summation is performed over all σ and π bonds.

The first term in equation (17) is responsible for the so-called 'kinetic exchange', which is related to the virtual electron transfer from one magnetic cation to another; the second term expresses 'semi-covalent exchange', which implies simultaneous formation of partially covalent bonds on both sides of the intermediate oxygen anion [18]. For the electronic configuration Fe^{3+}: $3d^5$, both mechanisms lead to the Fe^{3+}–O^{2-}–Fe^{3+} antiferromagnetic interaction. It is worth noting that the energies U and Δ in equation (17) mainly depend on the chemical nature of individual Fe^{3+} and O^{2-} cations; therefore, they will slightly change within one crystallographic class of perovskite iron oxides. Thus, the reason for the change in T_N in going from $RFeO_3$ to $TlFeO_3$ should be sought either in the change in the angular

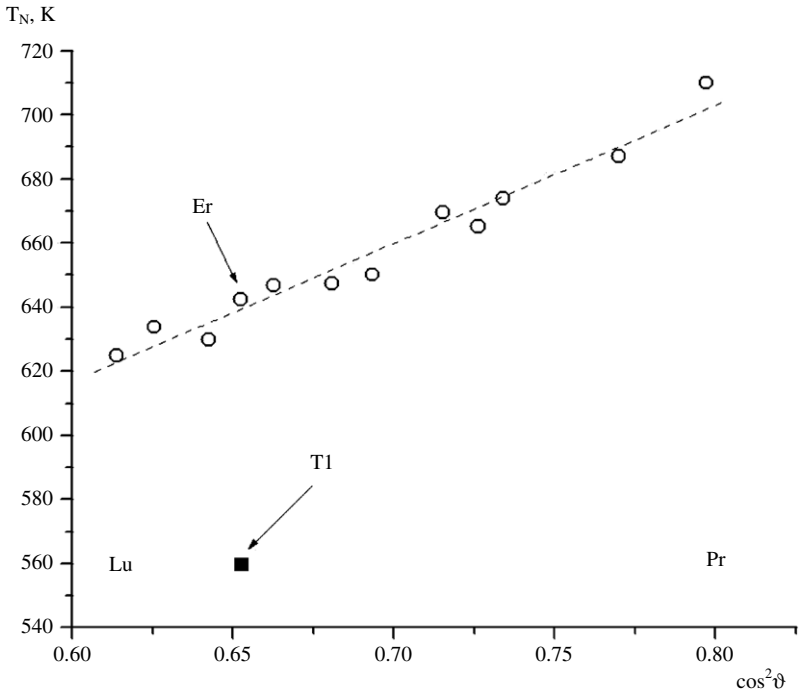

Figure 5. Evolution of T_N on $\cos^2\vartheta$ (where ϑ is the Fe–O–Fe superexchange angle) for $TlFeO_3$ and orthoferrites $RFeO_3$ (R = rare earth).

factor $\cos^2\vartheta$, related to the cooperative rotation of the $FeO_{6/2}$ polyhedra (steric factors), or in the change in the $b_{\sigma,\pi}$ parameters responsible for the degree of covalent transfer in the Fe^{3+}–O bonds (chemical factors).

Figure 5 shows the $T_N = f(\cos^2\vartheta)$ plot for the series of rare-earth orthoferrites $RFeO_3$ (where $\cos\vartheta = 1/3(\cos\vartheta_1 + 2\cos\vartheta_2)$); the T_N value for $TlFeO_3$ is given for comparison. This plot demonstrates that, in going from La to Lu, $T_N \propto \cos^2\vartheta$ decreases monotonically, which is evidence of the constancy of the $b_{\sigma,\pi}$ parameters within the entire $RFeO_3$ series. However, the T_N value for $TlFeO_3$ is considerably out of the common range for $RFeO_3$ (figure 5), which can be caused only by a decrease in covalence parameters $b_{\sigma,\pi}$, i.e., by weakening of the Fe^{3+}–O bonds. One possible reason for this effect is the indirect influence of Tl^{3+} cations on the parameters of the Fe–O chemical bonds. In the $TlFeO_3$ perovskite structure, the Tl^{3+} and Fe^{3+} cations are located in distorted TlO_{12} and FeO_6 polyhedra; therefore, their mutual influence can occur through indirect Tl^{3+}–O–Fe^{3+} bonds, in which the $2p_{x,y}$ atomic orbitals of O^{2-} anions concurrently participate in the formation of π bonds with the $3d_{xz,yz}$ orbitals of Fe^{3+} cations and of σ bonds with the 5s orbitals of Tl^{3+} cations (figure 6). Inasmuch as Tl^{3+} cations have high polarizability and rather high electron affinity [19], we may assume that the inductive redistribution of electrons in Tl ← O ← Fe chains will lead to the weakening of Fe–O bonds (a decrease in the b_π parameter) and, thus, to a decrease in the magnetic ordering temperature of the ferrite under consideration.

It is worth noting that the above qualitative explanation of the low T_N value for $TlFeO_3$ is additionally supported by the $T_N = f(c/\sqrt{2}a)$ plot in figure 7. Taking into account the above consideration of the $c/\sqrt{2}a$ ratio and the fact that the T_N value for $TlFeO_3$ fits well into the

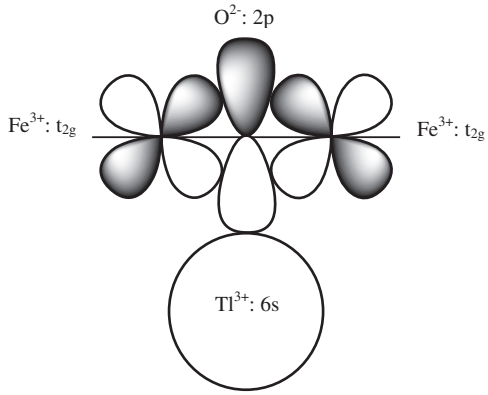

Figure 6. Scheme of the $d_{xy,yz}$ (Fe), $2p_z$ (O) and 6s (Tl) orbitals overlap in $TlFeO_3$ structure.

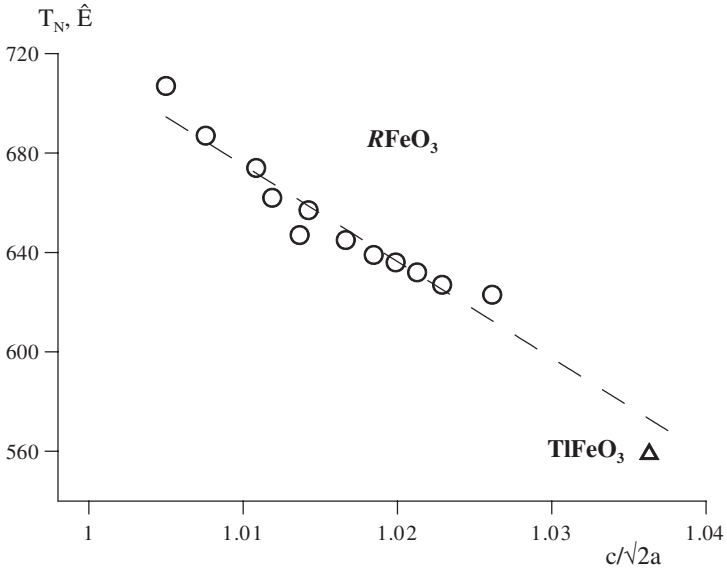

Figure 7. Evolution of T_N on the crystallographic axial ratio, $c/\sqrt{2}a$, for $TlFeO_3$ and orthoferrites $RFeO_3$ (R = rare earth).

general trend for the entire series of orthoferrites $RFeO_3$, we can draw a conclusion about the validity of our qualitative interpretation.

3.3. ^{57}Fe Mössbauer study of $TlFeO_3$ in the magnetic ordering range of temperature

The ^{57}Fe Mössbauer spectrum of $TlFeO_3$ at $T \ll T_N$ consists of one Zeeman sextet (figure 8). The isomer shift difference $\delta_{300\ K}(TlFeO_3) - \delta_{300\ K}(RFeO_3) \approx 0.09$ mm s^{-1} can be associated with the different covalence of the Fe–O chemical bonds in these systems.

The temperature dependence of the relative hyperfine magnetic field $\sigma_{Fe}(T) \equiv H_{Fe}(T)/H_{Fe}(0)$ (figure 7) is well expressed through the Brillouin function:

$$\sigma_{Fe}(T) = B_S\left\{\frac{2JS^2z}{kT}\sigma_{Fe}(T)\right\}, \tag{18}$$

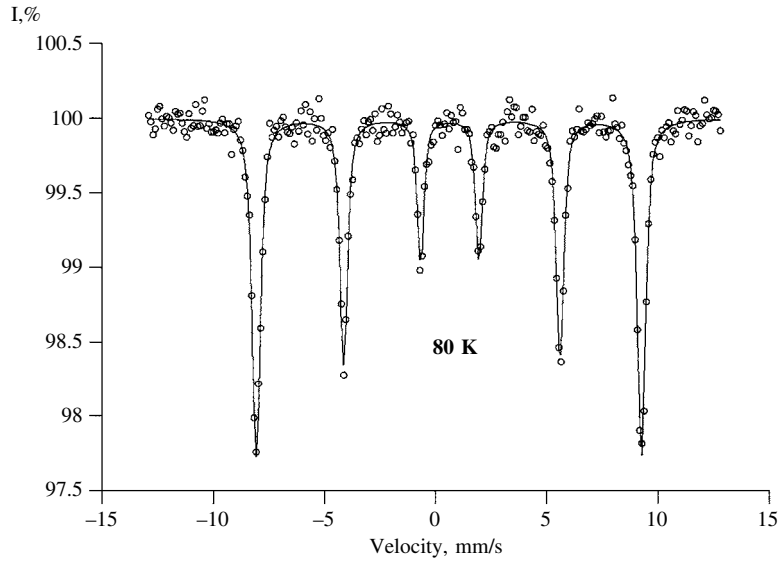

Figure 8. ^{57}Fe Mössbauer spectrum for $TlFeO_3$ at $T = 80$ K.

where $S = 5/2$ is the total spin of the Fe^{3+} cation, and the value of the hyperfine interaction integral (J) is calculated by substituting $T_N = 560$ K in (16). As a result of this dependence extrapolation at $T \to 0$, there was found a value of the 'saturation' field $H_{Fe}(0) = 535$ kOe, which is much lower in comparison with the values for the orthoferrites $RFeO_3$ [1].

Figure 10 gives the dependence of the experimental values $H_{Fe}(0) \propto \cos^2 \vartheta$ for the orthoferrites $RFeO_3$ and $TlFeO_3$. As was discussed for $RFeO_3$, a gradual change in $H_{Fe}(0)$ versus $\cos^2 \vartheta$ (which is due to the angle correlation of the overlap integrals participating in the formation of the Fe–O–Fe chemical bonds) is observed. In contrast, the value $H_{Fe}(0)$, as well as T_N for $TlFeO_3$, obviously falls out from the dependence $H_{Fe}(0) \propto \cos^2 \vartheta$, indicating the same nature for both deviations observed. In order to explain this phenomenon, we used a theoretical model for the dependence of the H_{Fe} value from the several parameters characterizing the Fe–O–Fe bonds involving the $3d_{\sigma,\pi}(Fe^{3+})$ and $2p_{\sigma,\pi}(O^{2-})$ atomic orbitals (see equation (17)).

On the basis of equations (12) and (13), the dependences between ΔH_{red}, ΔH_{STHF} and the value of the integrals (proportional to a part of the transferred charge density—due to the covalent effects along π (Fe–O) bond—formed by $2p_{x,y}$ orbitals of O^{2-} and t_{2g} orbitals of Fe^{3+} from the 'ideal' clusters $\{Fe(O_6Fe_6)\}$) can be obtained. From figure 11(a), it can be concluded that the change of the covalence for the Fe–O bonds influences the values of the ΔH_{red}, ΔH_{STHF} contributions in opposite ways (ΔH_{cov} is nearly constant). As a result, the final influence of the covalent effects on the total value H_{Fe} depends on the absolute values of the parameters $\{b_{4s}, b_{\sigma,\pi}, s_{\sigma,\pi}, \cos\vartheta\}$. To plot the dependences $\Delta H_{red}, \Delta H_{STHF} = f(b_\pi^2)$, the parameters which have been found earlier for the orthoferrites $RFeO_3$ have been used [15]. The chosen values for the angles correspond to: (i) $LaFeO_3$ with the least structural distortion among the $RFeO_3$ series ($\vartheta = 157.8°$); (ii) $LuFeO_3$ with the most important value for the structure distortion ($\vartheta = 141.8°$); (iii) $ErFeO_3$ ($\vartheta = 143.7°$) with the angle parameter which is the closest to that in $TlFeO_3$.

In figure 11(b) the $H_{Fe} = f(b_\pi^2)$ dependences are presented for these three chosen ϑ values. It can be observed that within the whole range of values of the Fe–O–Fe angles in

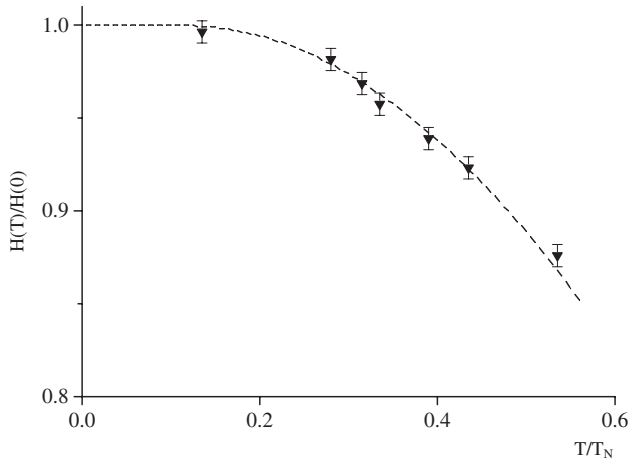

Figure 9. Temperature dependence of the hyperfine magnetic field H_{Fe} value at ^{57}Fe nuclei in $TlFeO_3$.

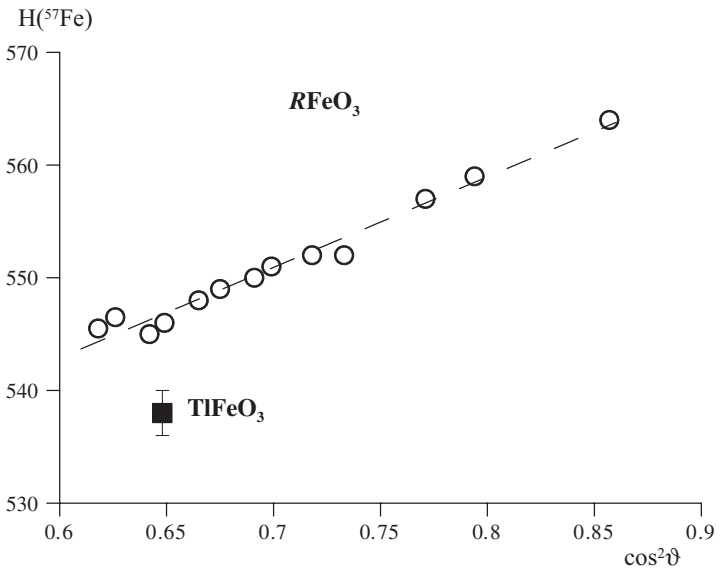

Figure 10. Dependence of the hyperfine magnetic field H_{Fe} value on $\cos^2\vartheta$ (where ϑ is the Fe–O–Fe superexchange angle) for $TlFeO_3$ and $RFeO_3$.

$RFeO_3$, the value of the hyperfine magnetic field H_{Fe} is gradually increased when the Fe–O bond covalence increases. Thus, the lower value of $H_{Fe}(0)$ for $TlFeO_3$ in comparison with $RFeO_3$ is really associated with the decrease of the Fe–O covalence degree (b_π^2) in the Fe–O–Fe chains. Taking into account that the same interactions are responsible for the magnitude of the exchange integral J_{FeOFe}, a decrease in the degree of covalence of the Fe–O bonds can also be a reason for the considerably lower Néel temperature for $TlFeO_3$ as compared to orthoferrites $RFeO_3$.

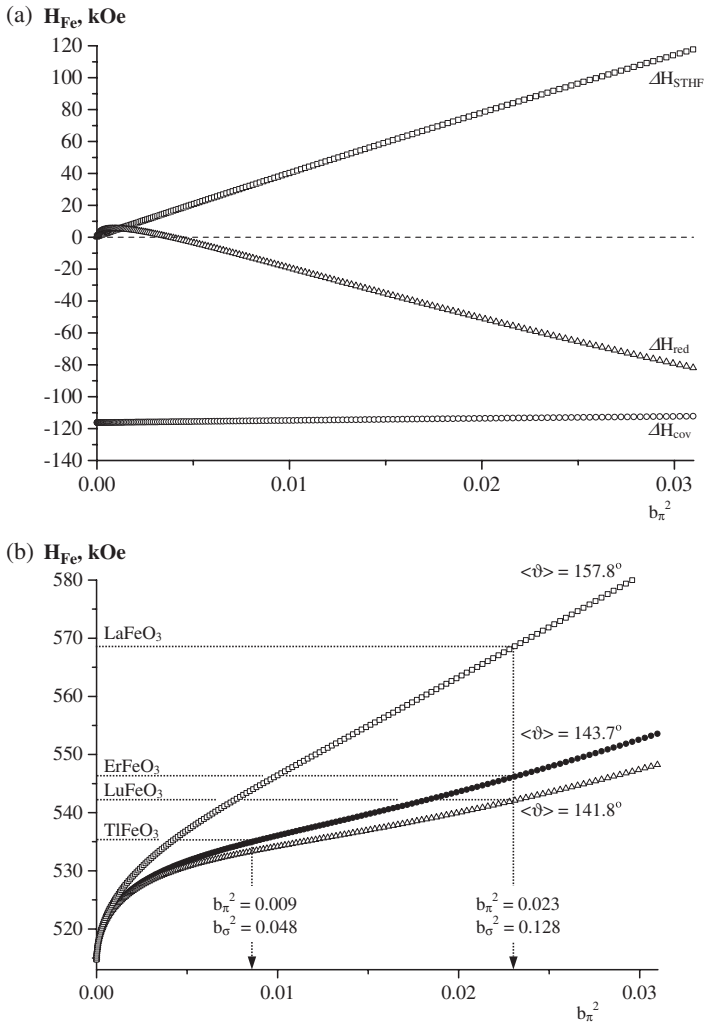

Figure 11. (a) Dependence of the ΔH_{red}, ΔH_{cov} and ΔH_{STHF} partial contributions in H_{Fe} for $TlFeO_3$; (b) dependence of the total field H_{Fe} for orthoferrites on the covalence parameter b_π^2.

3.4. ^{119}Sn magnetic hyperfine interactions in the $TlFe_{0.99}Sn_{0.01}O_3$ lattice

The ^{119}Sn Mössbauer spectra of $TlFe_{0.99}Sn_{0.01}O_3$, recorded at $T < T_N$, can be described as one Zeeman sextet (figure 12) with the isomer shift $\delta = 0.14 \pm 0.02$ mm s^{-1}, corresponding to tin cations in the formal oxidation state '+4' [10]. The narrow width of the sextet components ($\Gamma_{exp} = 0.98 \pm 0.01$ mm s^{-1}), close to the etalon value ($CaSnO_3$, $\Gamma = 0.92$ mm s^{-1}), is evidence of the equivalent crystallographic positions for the Sn^{4+} cations in the bulk of the ferrite structure.

The appearance of the magnetic hyperfine structure in the spectrum of the diamagnetic ^{119}Sn atoms is due to the splitting of the tin nuclei levels by the transferred magnetic hyperfine field (H_{Sn}) induced by the nearest magnetic iron cations. The absence of the non-magnetic component in the spectrum confirms the total stabilization of all tin cations in the bulk of the $TlFeO_3$ orthoferrite structure.

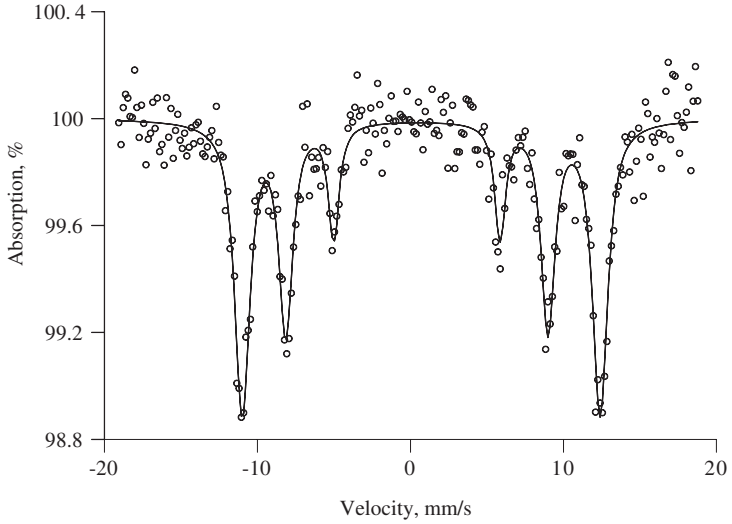

Figure 12. ^{119}Sn Mössbauer spectrum for $TlFe_{0.99}Sn_{0.01}O_3$ at $T = 80$ K.

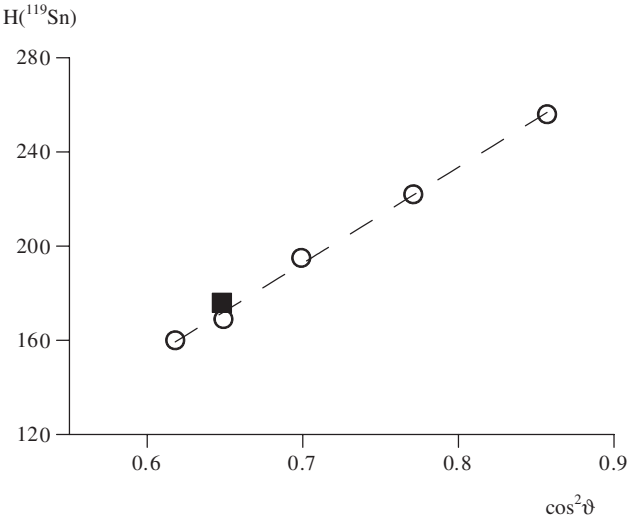

Figure 13. Dependence of the induced hyperfine field H_{Sn} at ^{119}Sn nuclei on the $\cos^2\vartheta$ in $RFe_{0.99}Sn_{0.01}O_3$ and $TlFe_{0.99}Sn_{0.01}O_3$.

The value $H_{Sn} = 167 \pm 2$ kOe ($T = 80$ K) is observed for $TlFe_{0.99}Sn_{0.01}O_3$. To compare the obtained value with that corresponding to $TFe_{0.99}Sn_{0.01}O_3$, the dependences H_{Sn} versus the angle Sn-O–Fe were plotted for the structure of $RFe_{0.99}Sn_{0.01}O_3$ [10] and $TlFe_{0.99}Sn_{0.01}O_3$ (figure 13). It was concluded through the resulting H_{Sn} values that the stabilization of the tin atoms in the ferrite structure is not accompanied by a difference between the (ϑ) angles corresponding to the Sn–O–Fe and Fe–O–Fe chains in the same matrix. The dependence $H_{Sn} = f(\cos^2\vartheta)$ shows that the H_{Sn} value in $TlFe_{0.99}Sn_{0.01}O_3$ is almost the same as that for $ErFe_{0.99}Sn_{0.01}O_3$ ($H_{Sn} = 166$ kOe), where the Sn–O–Fe angle is very close to that in the thallium ferrite. Thus, in contrast with the ^{57}Fe hyperfine fields, the H_{Sn} value is not very

sensitive to the parameters of the Fe–O bonds from the first coordination sphere of $\{Sn(O_6Fe_6)\}$ cluster, and mainly depends on the super-exchange angle values for the Sn–O–Fe bonds.

4. Conclusion

An accurate Mössbauer study of ^{57}Fe in the $TlFeO_3$ matrix compared to the $RFeO_3$ orthoferrites series (R = rare earth) has underlined the role of the electronic structure of the R^{3+} cation in the $RFeO_3$ perovskite with the *Pbnm* orthorhombic structural distortion. The specific electronic structure of $Tl^{3+}(4f^{14}5d^{10}6s^0)$ modifies the Tl^{3+}–O chemical bond due to its polarizing properties compared to the rare earth R^{3+}. Consequently two main phenomena are induced: (i) a structural distortion leading to four short Tl^{3+}–O bonds and (ii) a weakening of the competing Fe^{3+}–O chemical bond inducing a lower T_N value for $TlFeO_3$ compared to $ErFeO_3$ with approximately the same super-exchange ϑ (Fe–O–Fe) angle.

Acknowledgments

The authors would like to acknowledge financial support by the Russian Foundation for Basic Research (RFBR-CNRS Ref. No. 05-03-22003) and CNRS (PICS 3200). We also thank INTAS (YSF Ref. No. 03-55-2453) for supporting AB.

References

[1] Marezio M, Remeika J P and Dernier P D 1970 *Acta Crystallogr.* B **26** 2008
[2] Hayashi K, Demazeau J and Pouchard M 1981 *Rev. Chim. Minérale* **18** 148
[3] Torrance J B, Lacorre P, Nazzal A I, Ansaldo E G and Niedermayer C H 1992 *Phys. Rev.* B **45** 8209
[4] Goodenough J B and Raccah P M 1965 *J. Appl. Phys.* **36** 1031
[5] Alonso J A, Martinez-Lope M J, Casais M T, Aranda M A G and Fernandez-Diaz M T 1999 *J. Am. Chem. Soc.* **121** 4754
[6] Demazeau G, Kim S J, Presniakov I, Pokholok K, Baranov A, Sobolev A, Pankratov D and Ovanesyan N 2002 *J. Solid State Chem.* **168** 126
[7] Kim S J, Demazeau G, Presniakov I and Choy J H 2001 *J. Solid State Chem.* **161** 197
[8] Kim S J, Demazeau G, Presniakov I, Pokholok K, Sobolev A and Ovanesyan N 2001 *J. Am. Chem. Soc.* **123** 8127
[9] Eibschütz M E, Shtrikman S and Treves D 1967 *Phys. Rev.* **156** 562
[10] Lyubutin I S, Toshie O, Dmitrieva T V and Kazuo O 1974 *J. Phys. Soc. Japan* **36** 1006
[11] Gorodetsky G and Treves D 1964 *Phys. Rev.* A **135** 97
[12] Rusakov V S 1999 *Izv. Ross. Akad. Nauk.* **63** 1389
[13] van der Woude F and Sawatzky G A 1971 *Phys. Rev.* B **4** 3159
[14] Sawatzky G A, Geertswa W and Haas C 1976 *J. Magn. Magn. Mater.* **3** 37
[15] Watson R E 1958 *Phys. Rev.* **111** 1108
[16] Moskvin A S, Ovanesyan N S and Trukhtanov V A 1975 *Hyperfine Interact.* **1** 265
[17] Jaccarino V 1965 *Magnetism* vol II A (New York: Academic) p 307
[18] Goodenough J B 1963 *Magnetism and the Chemical Bond* (New York: Interscience)
[19] Sreltsov V A and Ishizawa N 1999 *Acta Crystallogr.* B **55** 1